

Universality of Avalanche Exponents in Plastic Deformation of Disordered Solids

Z. Budrikis,¹ D. Fernandez-Castellanos,² S. Sandfeld,² M. Zaiser,² and S. Zapperi^{3, 1, 4, 5}

¹*Institute for Scientific Interchange Foundation, Via Alassio 11/C, 10126 Torino*

²*WW8-Materials Simulation, FAU University of Erlangen-Nuremberg, Germany*

³*Center for Complexity and Biosystems, Department of Physics,*

University of Milano, via Celoria 26, 20133 Milano, Italy

⁴*CNR - Consiglio Nazionale delle Ricerche, Istituto per l'Energetica e le Interfasi, Via R. Cozzi 53, 20125 Milano, Italy*

⁵*Department of Applied Physics, Aalto University,*

P.O. Box 14100, FIN-00076 Aalto, Espoo, Finland

(Dated: May 17, 2022)

Plastic deformation of amorphous solids occurs by power law distributed slip avalanches whose universality is still debated. Interpreting results from experiments and molecular dynamics simulations is difficult due to limited statistical sampling, while existing elasto-plastic models are well understood but elasticity is only approximated by scalar fields. Here we introduce a fully tensorial mesoscale model for the elasto-plasticity of disordered media that is able to reproduce the wide variety of shear band patterns observed experimentally for different deformation modes. Slip avalanches are characterized by universal scaling laws that are largely independent on system dimensionality (2D vs 3D), boundary and loading conditions, and uni-or biaxiality of the stress state.

PACS numbers: 62.20.M-, 62.20.mm

Plasticity of both crystalline and amorphous materials is interesting from the point of view of statistical mechanics of complex systems because, during irreversible deformation under load, solids exhibit a rich variety of collective phenomena including spontaneous strain localization, intermittent dynamics and power-law distributed avalanches. This phenomenology overlaps with that seen in systems as diverse as ferromagnets exhibiting Barkhausen noise [1] and crack propagation [2–4], and a unified conceptual model for these problems is desirable. While there is consensus that plastic deformation in amorphous materials occurs via local reorganizations (shear transformation zones, STZ) [5–7], how these behave collectively is a topic that continues to receive considerable experimental and theoretical attention [8–28]. The interplay between disorder in local yield criteria and long range elastic interactions is captured by depinning-like models in which plastic deformation is mapped to the motion of an interface through a disordered medium [19, 22, 26, 29, 30]. The system undergoes a non-equilibrium depinning phase transition as the external drive approaches a critical value and universality implies the statistics of plastic avalanches to depend on only a few parameters such as dimensionality and interaction range. The nature of the universality class is, however, still controversial. Many groups have measured the avalanche size exponent τ in atomistic [23] or mesoscale simulations [8–10, 19, 22, 26, 29, 30] and in experiments [14, 16, 27, 28], and reported values range from 1.25 to 1.5 often with large error bars. Faced with such data, different groups have interpreted the results as either consistent with the mean-field exponent of $\tau = 3/2$ [27, 28] or not [19, 22, 26, 29, 30], and debate continues.

In addition to questions about universality, there remains a second important issue that has been almost completely overlooked in the published literature. Most

theoretical studies to date have focused on models which treat the plastic strain as a scalar variable — effectively assuming that shear occurs in a single direction only [8–10, 19, 22, 24, 26, 29–31]. This assumption which is inherent in all scalar models sits very uneasily with the statistically isotropic nature of amorphous solids, and makes such models appear more suited to single-slip crystal plasticity [32]. In case of finite samples subject to general loads, the assumption of a scalar strain occurring in response to a scalar load is quite obviously at variance with the tensor nature of stress and strain in continuum mechanics. This assumption makes it in principle impossible to model general deformation processes where stress is heterogeneous and multi-axial. Even if the applied stress is acting along a single stress axis, the models predict spontaneous strain localization and spatially fluctuating plastic strain fields, which implies that to ensure compatibility of deformation the stress field must locally be always multi-axial (see e.g. [33]). So one may legitimately ask what is the relevance of predictions derived from scalar models to real-world plasticity.

In the present letter we address this question by formulating a fully tensorial model of plasticity of disordered solids. We apply the model to both two- and three-dimensional problems, including finite samples, intrinsically heterogeneous deformation processes such as bending, and genuinely multi-axial loading conditions such as indentation. For all these systems we analyze the avalanche statistics in terms of the stress dependent distribution of avalanche sizes and determine the exponent τ which controls the power-law regime of the avalanche size distributions, the exponent σ which controls the divergence of the maximum avalanche size near the yield stress, and the exponent γ which connects duration and size of avalanches. Our simulations yield the surprising result that, under all these circumstances, these expo-

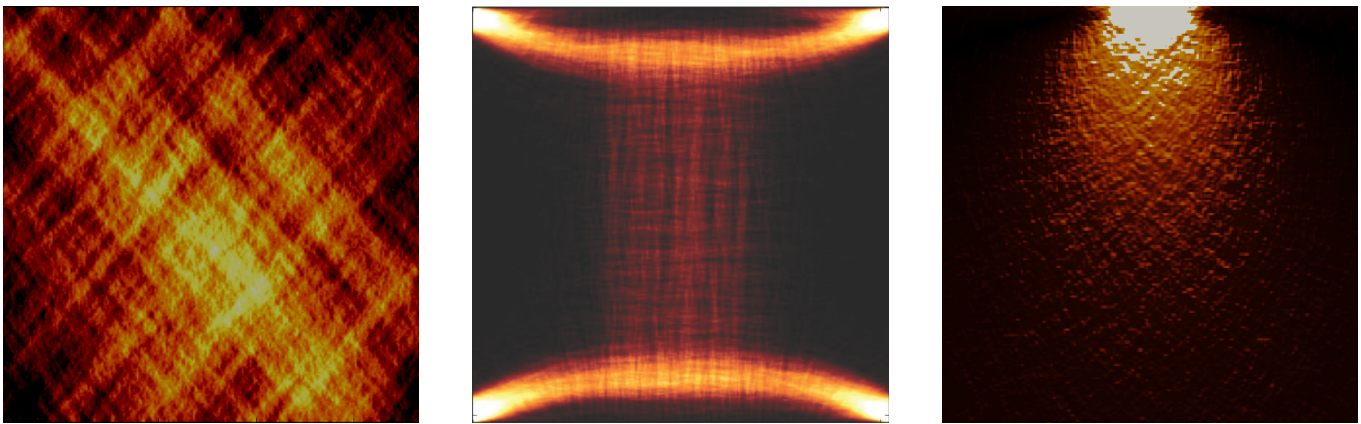


FIG. 1: Shear band patterns for different deformation modes; all system sizes 256×256 ; left: uniaxial tension, shear bands form under approximately 45 degrees to the tensile axis; centre: simple shear, the clamped boundary conditions cause strong stress concentrations in the specimen corners; right: indentation, shear bands follow intersecting circles as typical of secondary shear bands observed in indentation of bulk metallic glasses [34].

nents are the same - they neither depend on the nature of the stress and strain variables (scalar/uniaxial vs. tensorial/multiaxial), nor on the dimensionality of the system (2D vs. 3D), nor on the presence or absence of macroscopic strain gradients. Independence on loading conditions and dimensionality is suggestive of mean-field scaling, but in our case only the exponent σ agrees with the mean-field prediction $\sigma = 1/2$, while the other exponents are found to be significantly smaller than the predicted values $\tau = 3/2$ and $\gamma = 2$.

Our plasticity model is formulated in the spirit of rate-independent continuum plasticity with a J2/Von Mises type yield criterion, which we generalize in order to account for structural randomness and deformation occurring in localized, discrete events. We implement our simulations on a lattice consisting of D dimensional cubic elements and assign to each lattice element a local stress tensor Σ . From this we define a yield condition as

$$\Sigma_{\text{eq}} = \sqrt{(3/2)\Sigma' : \Sigma'} > \Sigma_y \quad (1)$$

where $\Sigma' = \Sigma - (1/D)\text{Tr}\Sigma\mathbf{I}$ is the deviatoric part of the stress tensor and \mathbf{I} is the rank-2-unit tensor in D dimensions. Plastic deformation occurs as soon as the equivalent stress at a lattice site exceeds the randomly assigned threshold Σ_y drawn from a uniform distribution over $[0, 1]$. Such elements are denoted as active.

Starting from zero plastic strain, we carry out our simulations by increasing the applied boundary displacements or tractions and evaluating the corresponding element stresses until the element \mathbf{r} closest to its yield threshold becomes active, thus triggering the first deformation event. Once an element is active, we increase the local plastic strain ϵ^{P} by an amount $\Delta\epsilon^{\text{P}} = \hat{\epsilon}\Delta\epsilon$ where the strain direction $\hat{\epsilon} = \Sigma'/\Sigma_{\text{eq}}$ is chosen to maximize the locally dissipated energy and $\Delta\epsilon$ is a fixed strain increment. We then re-compute the stresses and re-evaluate the yield condition for all elements. In gen-

eral, the stress re-distribution subsequent to a deformation event may cause other elements to become critical, thus producing an avalanche. During the avalanche, updates are performed in parallel with external boundary tractions/displacements kept fixed. This is repeated until no further elements become active and the avalanche stops. A new avalanche is then triggered by a renewed increase of the boundary displacements or tractions. The size S of an avalanche is defined as the total number of local strain increments, and its duration T is the number of parallel update steps performed.

For computing the stress field Σ from the plastic strain field ϵ^{P} and the external boundary conditions, we use two different methods, depending whether we are dealing with periodic boundary conditions mimicking an infinite system, or with a finite sample with imposed boundary displacements and/or tractions. In the former case we consider stress and strain only at the element center-points which form a cubic grid with periodic boundary conditions. We use a Green's function method to evaluate the stress associated with the spatially heterogeneous plastic strain by spatial convolution. In Fourier space

$$\Sigma_{ij}^{\text{int}}(\mathbf{q}) = \mathbf{G}_{ijkl}(\mathbf{q})\epsilon_{kl}^{\text{P}}(\mathbf{q}). \quad (2)$$

The interaction kernel \mathbf{G} is obtained by treating the plastic strain of an element as the strain of an Eshelby inclusion of vanishing volume located at the element centre-point. For such an inclusion the stress field is known analytically, and continuing this solution periodically with period L allows us to use double Fast Fourier Transform to evaluate the overall internal stress field that arises from superposition of all element stresses. We then superimpose a spatially homogeneous 'external' stress field Σ^{ext} which is understood to arise from remote boundary tractions applied to the infinite contour. When dealing with finite samples, we use standard finite element methodology to solve the elastic-plastic problem with the specified boundary conditions (for details of the FEM implemen-

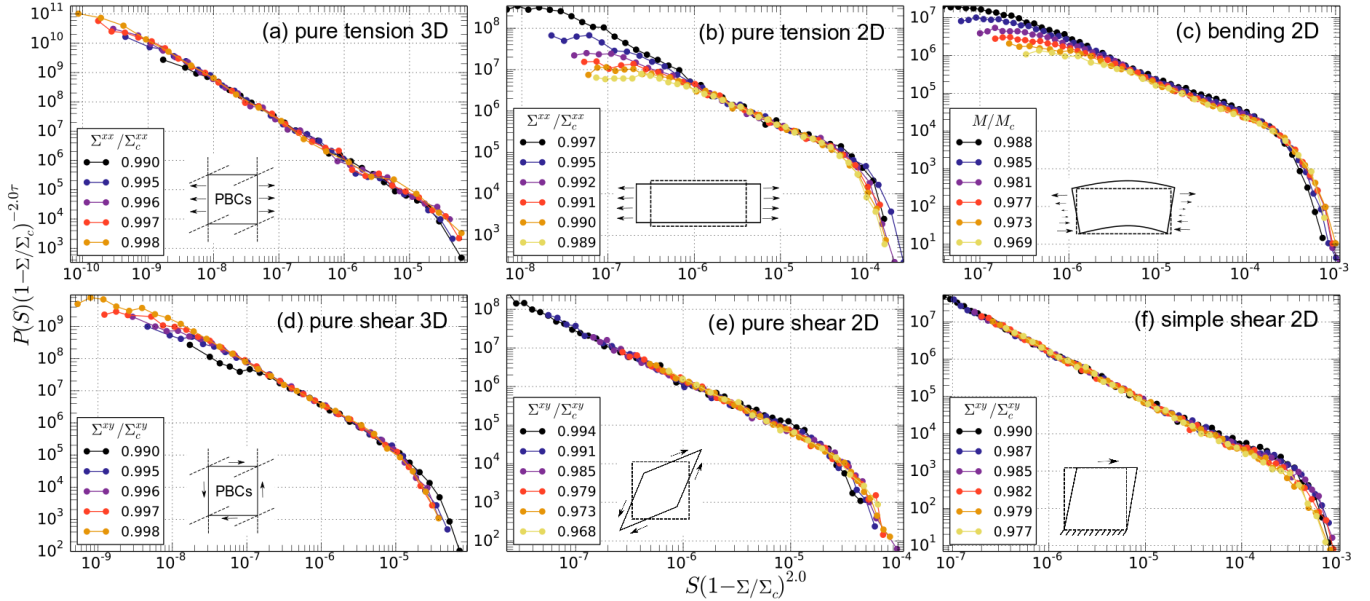


FIG. 2: Avalanche size distributions for different deformation modes; each graph represents distributions pertaining to different stress levels as indicated in the legends and rescaled using the exponents $1/\sigma = 2.0$ and exponent $\tau = 1.35$ (except for panel c) where $\tau = 1$). a) Uniaxial tension in 3D, periodic BC ($\tau = 1.35$). b) Uniaxial tension in 2D, free side surfaces; c) Bending in 2D with bending moment M applied to end surfaces. d) Pure shear in 3D, periodic BC. e) Pure shear in 2D, free side surfaces with uniform applied shear tractions. f) Simple shear in 2D with shear tractions applied to clamped top and bottom surfaces.

tation in context of a scalar model, see [30]). We use four-node linear elements of square shape. Each element is associated with an element stress that is evaluated as the average stress over the element. An active element experiences a plastic strain increment that is homogeneous over the element and zero elsewhere. Both models are matched by ensuring that the plastic strain field of the point-like Eshelby inclusion, integrated over the element, has the same value as the homogeneous element strain in the finite element model.

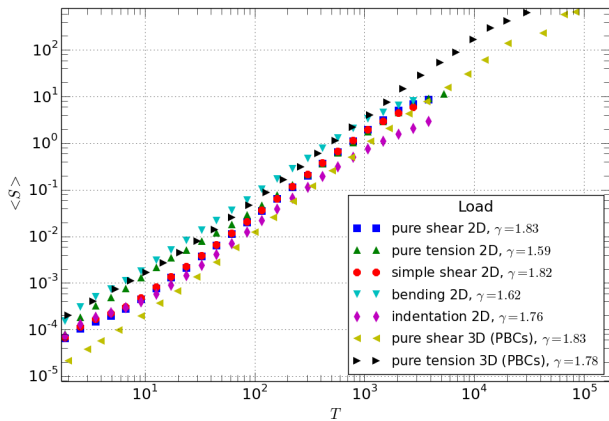


FIG. 3: Avalanche size vs. avalanche duration for different deformation conditions and space dimensionalities

Simulations have been performed in both two and three

dimensions, considering both macro-homogeneous deformation modes (uniaxial tension with free surfaces and applied tensile tractions, pure shear) and, in 2D, also macro-heterogeneous deformation modes such as simple shear with clamped top and bottom surfaces, bending, and indentation. Various system sizes were considered ranging up to 64^3 elements for the 3D model and 256^2 elements for the 2D finite element calculations. In all cases the plastic strain field organizes into localization patterns (shear bands) which approximately follow the directions of maximum shear stress as illustrated in Figure 1 for the cases of uniaxial tension and two bi-axial and macro-heterogeneous deformation modes, namely simple shear with clamped top and bottom surfaces and indentation. The results reveal a strong universality of the avalanche exponent $\tau = 1.35 \pm 0.05$ which is not only independent on dimensionality (2D vs. 3D) but also does not depend on the description of stress (scalar vs. tensor) nor whether the stress field is homogeneous and uniaxial (pure shear, pure tension) or inhomogeneous and biaxial (simple shear). Pure tension and pure shear produce identical results, which indicates that the avalanche exponent is not influenced by the presence or absence of hydrostatic stresses (pure tension adds a hydrostatic stress contribution), by boundary conditions, or by the orientation of the simulation grid (deviatoric stresses are in both cases equivalent but the directions of shear differ by 45 degrees). The size S_{\max} of the largest avalanches diverges like $S_{\max} \propto (\Sigma_c - \Sigma)^{-1/\sigma}$ as the system average of the equivalent stress Σ approaches a non-universal

critical value Σ_c ; accordingly, the distributions exhibit the scaling form $p(S) = u^{-\tau}\Psi(u)$ where $u = S/S_{\max}$. The exponent $1/\sigma = 2 \pm 0.1$ exhibits the same strong universality as the avalanche exponent τ . Irrespective of stress and contrary to claims in the literature [29] we do not find any discernable dependency of S_{\max} on system size. A third universal exponent γ defines the relationship between avalanche duration T and avalanche size $S \propto T^\gamma$. To determine this exponent we define the duration of an avalanche as the number of simultaneous updates required from the begin of the avalanche to the moment when all elements are stable again. Also here we find strong universality with an exponent $\gamma = 1.75 \pm 0.2$ (Fig. 3).

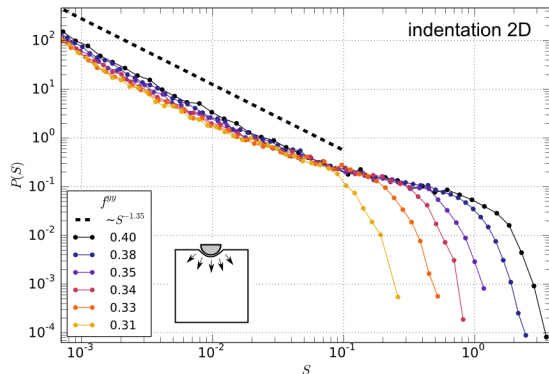


FIG. 4: Avalanche size distributions for indentation with a spherical indenter. Here f denotes the force acting on the indenter divided by the indenter cross section. The dashed line represents an avalanche exponent $\theta = 1.35$

There are limits to universality. In some deformation processes where the deformation state is intrinsically heterogeneous, such as bending or indentation, we find de-

viations from the above described behavior. Thus, in bending, we see a reduced exponent $\tau = 1$ and also a reduced value of γ whereas the exponent $1/\sigma \approx 2$ remains unchanged. The critical stress Σ_c here corresponds to the limiting value of the bending moment M_c at which the deforming specimen becomes fully plastic, with opposite directions of deformation above and below the neutral axis. Whereas bending deformation corresponds to a heterogeneous but uniaxial stress state, the stress state in indentation is both heterogeneous and multi-axial. Moreover, in this case the fraction of the simulated specimen that actually undergoes plastic deformation is increasing monotonically with increasing force acting on the indenter. In this case, no critical stress Σ_c can be defined and the avalanche size distributions are, in the regime of the largest avalanches, not well described by truncated power laws (see Fig. 4).

Our results show several intriguing features. First, we observe the fact that the fully tensorial model produces the same avalanche exponent as previously introduced scalar plasticity models. This is comforting and provides a certain *a posteriori* justification of the use of scalar models. At the same time we note that the exponents σ and γ differ somewhat from the value found for the scalar model [30]. The independence of all exponents on system dimension seems to suggest mean-field behavior, however, even though the value of $1/\sigma \approx 2$ matches the expectation for mean-field depinning, the exponents $\tau = 1.35$ and $\gamma = 1.75$ differ from the predictions $\tau = 1.5$ and $\gamma = 2$ derived from a mean-field theory of the depinning transition [13]. A possible explanation for this may be related to the fact that the long-range elastic interactions associated with elasto-plasticity are not associated with a positively definite elastic kernel, invalidating a crucial assumption of the renormalization group theory on which our current understanding of universality classes related to depinning phenomena [35] is based.

-
- [1] G. Durin and S. Zapperi, in *The Science of Hysteresis*, edited by G. Bertotti and I. Mayergoyz (Elsevier, Amsterdam, 2006), vol. 2, pp. 181–267.
 - [2] D. Bonamy, S. Santucci, and L. Ponson, *Phys. Rev. Lett.* **101**, 045501 (2008), URL <http://link.aps.org/doi/10.1103/PhysRevLett.101.045501>.
 - [3] L. Laurson, S. Santucci, and S. Zapperi, *Phys. Rev. E* **81**, 046116 (2010), URL <http://link.aps.org/doi/10.1103/PhysRevE.81.046116>.
 - [4] L. Laurson, X. Illa, S. Santucci, K. T. Tallakstad, K. J. Måløy, and M. J. Alava, *Nature communications* **4** (2013).
 - [5] A. Argon and H. Kuo, *Materials Science and Engineering* **39**, 101 (1979), ISSN 0025-5416, URL <http://www.sciencedirect.com/science/article/pii/0025541679901745>.
 - [6] A. Argon and L. Shi, *Acta Metallurgica* **31**, 499 (1983), ISSN 0001-6160, URL <http://www.sciencedirect.com/science/article/pii/000161608390038X>.
 - [7] M. L. Falk and J. S. Langer, *Phys. Rev. E* **57**, 7192 (1998), URL <http://link.aps.org/doi/10.1103/PhysRevE.57.7192>.
 - [8] J.-C. Baret, D. Vandembroucq, and S. Roux, *Phys. Rev. Lett.* **89**, 195506 (2002), URL <http://link.aps.org/doi/10.1103/PhysRevLett.89.195506>.
 - [9] G. Picard, A. Ajdari, L. Bocquet, and F. m. c. Lequeux, *Phys. Rev. E* **66**, 051501 (2002), URL <http://link.aps.org/doi/10.1103/PhysRevE.66.051501>.
 - [10] G. Picard, A. Ajdari, F. m. c. Lequeux, and L. Bocquet, *Phys. Rev. E* **71**, 010501 (2005), URL <http://link.aps.org/doi/10.1103/PhysRevE.71.010501>.
 - [11] E. A. Jagla, *Phys. Rev. E* **76**, 046119 (2007), URL <http://link.aps.org/doi/10.1103/PhysRevE.76.046119>.
 - [12] Z. W. Shan, J. Li, Y. Q. Cheng, A. M. Minor, S. A. Syed Asif, O. L. Warren, and E. Ma, *Phys. Rev. B* **77**, 155419 (2008), URL <http://link.aps.org/doi/10.1103/PhysRevB.77.155419>.
 - [13] K. A. Dahmen, Y. Ben-Zion, and J. T. Uhl, *Phys. Rev.*

- Lett. **102**, 175501 (2009), URL <http://link.aps.org/doi/10.1103/PhysRevLett.102.175501>.
- [14] G. Wang, K. Chan, L. Xia, P. Yu, J. Shen, and W. Wang, *Acta Materialia* **57**, 6146 (2009), ISSN 1359-6454, URL <http://www.sciencedirect.com/science/article/pii/S1359645409005527>.
- [15] E. R. Homer, D. Rodney, and C. A. Schuh, *Phys. Rev. B* **81**, 064204 (2010), URL <http://link.aps.org/doi/10.1103/PhysRevB.81.064204>.
- [16] B. A. Sun, H. B. Yu, W. Jiao, H. Y. Bai, D. Q. Zhao, and W. H. Wang, *Phys. Rev. Lett.* **105**, 035501 (2010), URL <http://link.aps.org/doi/10.1103/PhysRevLett.105.035501>.
- [17] B. A. Sun and W. H. Wang, *Applied Physics Letters* **98**, 201902 (2011), URL <http://scitation.aip.org/content/aip/journal/apl/98/20/10.1063/1.3592249>.
- [18] K. Martens, L. Bocquet, and J.-L. Barrat, *Phys. Rev. Lett.* **106**, 156001 (2011), URL <http://link.aps.org/doi/10.1103/PhysRevLett.106.156001>.
- [19] M. Talamali, V. Petäjä, D. Vandembroucq, and S. Roux, *Phys. Rev. E* **84**, 016115 (2011), URL <http://link.aps.org/doi/10.1103/PhysRevE.84.016115>.
- [20] M. Talamali, V. Petj, D. Vandembroucq, and S. Roux, *Comptes Rendus Mcanique* **340**, 275 (2012), ISSN 1631-0721, recent *Advances in Micromechanics of Materials*, URL <http://www.sciencedirect.com/science/article/pii/S1631072112000472>.
- [21] B. Sun, S. Pauly, J. Tan, M. Stoica, W. Wang, U. Khn, and J. Eckert, *Acta Materialia* **60**, 4160 (2012), ISSN 1359-6454, URL <http://www.sciencedirect.com/science/article/pii/S1359645412002698>.
- [22] Z. Budrikis and S. Zapperi, *Phys. Rev. E* **88**, 062403 (2013), URL <http://link.aps.org/doi/10.1103/PhysRevE.88.062403>.
- [23] K. M. Salerno and M. O. Robbins, *Phys. Rev. E* **88**, 062206 (2013), URL <http://link.aps.org/doi/10.1103/PhysRevE.88.062206>.
- [24] A. Nicolas, K. Martens, L. Bocquet, and J.-L. Barrat, *Soft Matter* **10**, 4648 (2014), URL <http://dx.doi.org/10.1039/C4SM00395K>.
- [25] J. Lin, A. Saade, E. Lerner, A. Rosso, and M. Wyart, *EPL (Europhysics Letters)* **105**, 26003 (2014), URL <http://stacks.iop.org/0295-5075/105/i=2/a=26003>.
- [26] J. Lin, E. Lerner, A. Rosso, and M. Wyart, *Proceedings of the National Academy of Sciences* **111**, 14382 (2014).
- [27] J. Antonaglia, W. J. Wright, X. Gu, R. R. Byer, T. C. Hufnagel, M. LeBlanc, J. T. Uhl, and K. A. Dahmen, *Phys. Rev. Lett.* **112**, 155501 (2014), URL <http://link.aps.org/doi/10.1103/PhysRevLett.112.155501>.
- [28] J. Antonaglia, X. Xie, G. Schwarz, M. Wraith, J. Qiao, Y. Zhang, P. K. Liaw, J. T. Uhl, and K. A. Dahmen, *Scientific Reports* **4**, 4382 (2014).
- [29] J. Lin, T. Gueudre, A. Rosso, and M. Wyart, *Phys. Rev. Lett.* **115**, 168001 (2015), URL <http://link.aps.org/doi/10.1103/PhysRevLett.103.065501>.
- [30] S. Sandfeld, Z. Budrikis, S. Zapperi, and D. Fernandez Castellanos, *Journal of Statistical Mechanics: Theory and Experiment* **2015**, P02011 (2015), URL <http://stacks.iop.org/1742-5468/2015/i=2/a=P02011>.
- [31] K. Martens, L. Bocquet, and J.-L. Barrat, *Soft Matter* **8**, 4197 (2012).
- [32] M. Zaiser and P. Moretti, *Journal of Statistical Mechanics: Theory and Experiment* **2005**, P08004 (2005), URL <http://stacks.iop.org/1742-5468/2005/i=08/a=P08004>.
- [33] S. Sandfeld and M. Zaiser, *Journal of Statistical Mechanics: Theory and Experiment* **2014** (2014), ISSN 17425468, URL <http://iopscience.iop.org/1742-5468/2014/3/P03014/>.
- [34] K. Chen and J. Lin, *Int. J. Plasticity* **26**, 1645 (2010).
- [35] P. Le Doussal, K. J. Wiese, and P. Chauve, *Phys. Rev. B* **66**, 174201 (2002), URL <http://link.aps.org/doi/10.1103/PhysRevB.66.174201>.